Albedo Retrieval From Sentinel-2 by New Narrow-to-Broadband Conversion Coefficients

Stefania Bonafoni, *Member IEEE*, and Aliihsan Sekertekin

***Abstract*— Surface albedo in the rural and urban environment is one of the most influencing parameters in the evaluation of the radiative forcing of the land surface. Satellite remote sensing is an efficient tool for surface broadband albedo estimation with various spatial resolutions. Different retrieval algorithms were proposed and tested in the literature. This letter focuses on the narrow-to-broadband conversion algorithm applied to Sentinel-2 reflective data, using its best spatial resolution (10 m). New narrow-to-broadband coefficients for albedo retrieval were computed. Their accuracy was tested with ground-based measurements in two different environments and compared with another algorithm introduced in the literature. The application of these coefficients for the albedo estimation requires the assumption of Lambertian surface and clear sky conditions. The first test was performed on six field stations of the Surface Radiation Budget Network (SURFRAD), and the second test was carried out within an urban area (Perugia, Central Italy), to better evaluate the impact of the spatial resolution on the albedo estimation from spaceborne sensors. The obtained root mean square error (RMSE) for the two tests presented very good values for both algorithms (around 0.02), with a slightly better performance of the proposed coefficients, especially for the higher albedo values. In the urban test, the retrieved albedo from Sentinel-2 with a 10-m pixel size provided considerably better results than the Landsat 8 estimation (30-m), highlighting the benefit of using a finer resolution in heterogeneous environments.**

***Index Terms*— Albedo, narrow-to broadband conversion, Sentinel-2, Surface Radiation Budget Network (SURFRAD), urban environment.**

I. Introduction

SURFACE albedo is a fundamental driver in the quantification of the radiative forcing of the Earth's surface, and therefore, of the Earth Radiation Budget [1]. Albedo measurements are useful in the investigation and modeling of the energy transfer between the land surface and atmosphere [2]. Surface albedo varies as a result of solar illumination, snowfall, flooding, vegetation growth, and natural or anthropogenic changes of land covers. Spaceborne remote sensing techniques are an efficient tool for deriving and monitoring surface broadband albedo with various spatial and temporal resolutions [3]–[5].

Manuscript received October 15, 2019; revised December 17, 2019 and January 10, 2020; accepted January 13, 2020. Date of publication January 29, 2020; date of current version August 28, 2020. This work was supported by the Fondo di Ricerca di Base through the University of Perugia. *(Corresponding author: Stefania Bonafoni.)*

Stefania Bonafoni is with the Engineering Department, University of Perugia, 06123 Perugia, Italy (e-mail: stefania.bonafoni@unipg.it).

Aliihsan Sekertekin is with the Department of Geomatics Engineering, Cukurova University, 01330 Adana, Turkey (e-mail: aliihsan_sekertekin@hotmail.com).

Color versions of one or more of the figures in this letter are available online at http://ieeexplore.ieee.org.

Digital Object Identifier 10.1109/LGRS.2020.2967085

Broadband albedo is defined as the ratio of the reflected flux density (W/m^2) to the incident flux density, referred to the whole spectrum of solar radiation (0.3–3 μm), also named shortwave (SW) albedo. Narrowband albedo is the albedo over a narrow range of wavelengths.

Since the 1990s, several letters addressed the albedo estimation challenge from satellite measurements, as detailed in the review letter of Qu *et al.* [6]. Algorithms for estimating surface broadband albedo from satellite observations include a) narrow-to-broadband conversions; b) bidirectional reflectance distribution function (BRDF) angular modeling; c) direct-estimation algorithm; and d) algorithms for geostationary satellite data [6]. They were developed and improved across the years, and a comprehensive literature review and discussion on these four categories are thoroughly reported in [6]. Currently, the first two categories a) and b) are the most commonly used ones in the literature. Algorithms in a) are suitable when the land surface is roughly assumed as Lambertian, i.e., the reflectance is considered isotropic from different solar/view angles. On the other hand, BRDF angular modeling b) is suitable to describe the reflectance anisotropy of the surfaces and relies on multiangular satellite observations [7].

Among the four previous algorithm categories, this letter focuses on the narrow-to-broadband conversion method. By considering the previous studies, it was initially developed using Landsat data [8]. Then, this method was applied to the Advanced Very High Resolution Radiometer (AVHRR) [9], [10], and Meteosat [11]. Liang [4] improved the former studies by providing easy-to-use conversion coefficients for albedo estimation for different satellite sensors. The Liang narrow-to-broadband coefficients were computed by regressions using extensive radiative transfer simulations and spectral reflectance libraries. These coefficients are widely utilized, and [4] can be considered as a milestone in this topic. A further narrow-to-broadband albedo conversion for Landsat sensors and Moderate Resolution Imaging Spectroradiometer (MODIS) is described in the letter of Tasumi *et al.* [12]. They applied an approach integrating at-surface narrowband reflectances with weighting coefficients representing the solar radiation fraction within each satellite spectral band. Methods in [4] and [12] do not consider Sentinel-2, because formulated much earlier than the mission development. Sentinel-2 has been operational since 2015, observing reflected radiances even at 10 m spatial resolution and thus providing an improvement with respect to Landsat missions (30 m). Recently, some letters proposed the albedo retrieval from Sentinel-2 using the same coefficients computed for the Landsat Enhanced Thematic Mapper (ETM+) by Liang in [4], directly applied to Sentinel-2 Multispectral Instrument (MSI) bands [13]–[15].

However, this approach suffers from the different bandwidths and central wavelengths of the sensor channels

1545-598X © 2020 IEEE. Personal use is permitted, but republication/redistribution requires IEEE permission.
See https://www.ieee.org/publications/rights/index.html for more information.

Authorized licensed use limited to: UNIVERSIDAD CARLOS III MADRID. Downloaded on October 05,2021 at 13:20:51 UTC from IEEE Xplore. Restrictions apply.

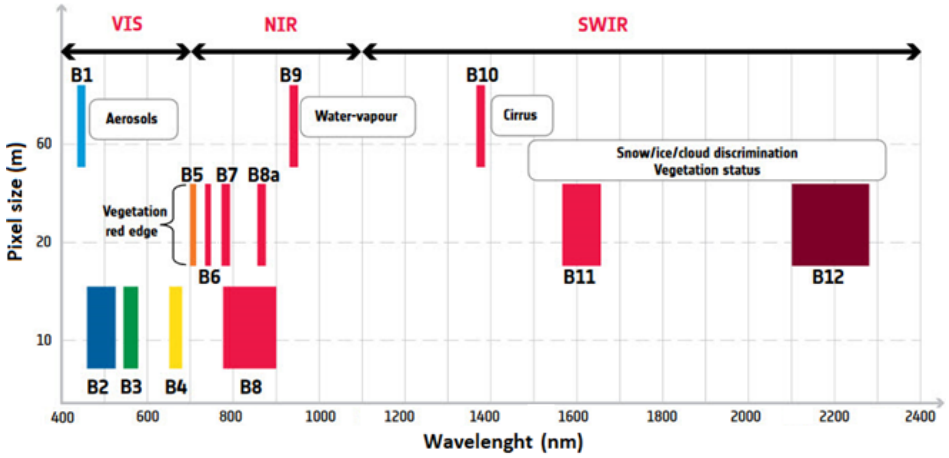

Fig. 1. Sentinel-2 MSI channels (B1–B13): pixel size (m) versus wavelength (nm). Source: [18].

of the two satellites. On the contrary, Li *et al.* [16] computed the narrow-to-broadband coefficients for Sentinel-2 MSI by applying the same regression methodology of Liang [4].

In this letter, new narrow-to-broadband conversion coefficients for Sentinel-2 albedo retrieval in clear sky conditions were computed by applying the methodology of Tasumi *et al.* [12] to the MSI channels. Their accuracy was tested by ground measurements in two different environments and compared with the approach of Li *et al.* [16]. For the application of the narrow-to-broadband conversion algorithm, the surface of the test sites is assumed as Lambertian. The best MSI spatial resolution (10 m) was used, exploiting a resolution enhancement method applied to the coarser pixels. In the first test, the albedo ground measurements of six field stations of the Surface Radiation Budget Network (SURFRAD) were considered. The second test was carried out with *in situ* measurements within an urban area (Perugia, Central Italy), to appreciate better the benefit of retrieving the albedo from spaceborne sensors with 10-m pixel size.

II. Methodology

A. Sentinel-2 Specifications

Sentinel-2 is a multispectral imaging mission with two identical satellites (Sentinel-2A and Sentinel-2B) placed in the same sun-synchronous orbit at a mean altitude of 786 km, with a high revisit time of two to three days at mid-latitudes. Sentinel-2A was launched on 23 June 2015, and Sentinel-2B on 7 March 2017. MSI onboard of both Sentinel-2 platforms [17] measures in a 20.6° field of view the Earth's reflected radiance in 13 spectral bands in the visible/near-infrared (VNIR) and SW infrared range (SWIR), at different spatial resolutions (10–60 m) (Fig. 1). Different level products are available for users: in this letter, Level-2A products providing Bottom-Of-Atmosphere (BOA) reflectances were used for albedo retrieval. Level-2A data are radiometrically and geometrically corrected, including orthorectification, projected into the UTM-WGS 84 coordinate system. BOA reflectances are also atmospherically corrected, as described in [17].

B. Narrow-to-Broadband Albedo Retrieval

From MSI BOA reflectances, an easy-to-use algorithm for albedo estimation is developed here for Sentinel-2. It follows the strategy used for Landsat and MODIS data in [12], for typical cloud-free, snow-free, low-haze conditions, and sensor view angles less than 20°. The broadband surface albedo α is estimated by integration of narrowband reflectances across the SW spectrum, as

$$\alpha = \sum_{B=1}^{N} \rho_B \cdot w_B \tag{1}$$

where ρ_B is the surface reflectance for a specific band B of MSI, and w_B is the weighting coefficient computed as

$$w_B = \frac{\int_{L_B}^{U_B} R_{s\lambda} \cdot d\lambda}{\int_{0.3}^{3} R_{s\lambda} \cdot d\lambda} \tag{2}$$

where $R_{s\lambda}$ is the at-surface spectral solar radiation at wavelength λ (μm), U_B and L_B are the upper- and lower-wavelength limits assigned to the selected band B of Sentinel-2 (Table I). Therefore, w_B represents the weight of the portion of the at-surface solar radiation encompassing the spectral range of a specific band B. Endpoints of integration were chosen as 0.3–3 μm, which covers almost all the at-surface solar radiation, since downward fluxes beyond this range are negligible. As listed in Table I, in order to exploit the best spatial resolution (10 m), the bands B2, B3, B4, and B8 were selected for the VNIR spectral range, and the window bands B11 and B12 for the SWIR. These SWIR bands, with native 20-m pixel size, were super-resolved at 10 m using the resolution enhancement method in [19] and delivered as a plugin for the Sentinel Application Platform (SNAP) [17]. The direct application of w_B to the observed MSI reflectances for SW albedo estimation is suitable for surfaces assumed as Lambertian.

In the w_B computation, the inclusion of the missing wavelength regions between bands provides a more

TABLE I
MSI Spectral Bands (Similar for Sentinel-2A and -2B [17]), U_B and L_B Limits, and Weighting Coefficients w_B

MSI Channels	Central wavelength (μm)	Bandwidth (μm)	U_B and L_B (μm)	w_B
B2	0.492	0.066	0.3 – 0.533	0.2266
B3	0.559	0.036	0.533 – 0.614	0.1236
B4	0.665	0.031	0.614 – 0.730	0.1573
B8	0.833	0.106	0.730 – 1.226	0.3417
B11	1.612	0.092	1.226 – 1.880	0.1170
B12	2.194	0.180	1.880 – 3.00	0.0338

Authorized licensed use limited to: UNIVERSIDAD CARLOS III MADRID. Downloaded on October 05,2021 at 13:20:51 UTC from IEEE Xplore. Restrictions apply.

TABLE II

SURFRAD STATIONS USED FOR THE ACCURACY ASSESSMENT OF THE SENTINEL-2 ALBEDO RETRIEVAL IN THE PERIOD 2018-2019. A TOTAL OF 42 SENTINEL-2 CLEAR SKY SCENES WERE CONSIDERED

Site Name	Site ID	Latitude	Longitude	Land Cover Type	Scenes #
Bondville, Illinois	BND	40.05192° N	88.37309° W	Cropland	7
Fort Peck, Montana	FPK	48.30783° N	105.1017° W	Grassland	8
Goodwin Creek, Mississippi	GWN	34.25470° N	89.87290° W	Cropland/Natural Vegetation Mosaic	11
Table Mountain, Boulder, Colorado	TBL	40.12498° N	105.2368° W	Sparse Grassland	6
Penn. State Univ., Pennsylvania	PSU	40.72012° N	77.93085° W	Cropland	3
Sioux Falls, South Dakota	SXF	43.73403° N	96.62328° W	Grassland	7

theoretically valid evaluation of the SW albedo [12]. The regions between sensor bands were divided midway between band limits assuming that reflectance in these regions can be approximated by linear interpolation of reflectances for adjacent bands [12] (Table I).

The Simple Model of the Atmospheric Radiative Transfer of Sunshine (SMARTS) software [20] was used for the computation of cloud-free solar radiation levels at the surface in (2). The obtained weights w_B for the Midlatitude reference atmosphere are reported in Table I. Hereafter, the albedo computation with these coefficients is named "S2_wgt."

The other narrow-to-broadband conversion method (1) for Sentinel-2 proposed by Li *et al.* [16] is hereafter named "S2_reg." It uses regression coefficients based on radiative transfer simulations and spectral reflectance libraries of various surface types, as in Liang [4]. In Section III, S2_wgt and S2_reg accuracies will be compared.

C. Ground Measurements

Two tests were considered for the assessment of the accuracy of S2_wgt and S2_reg methods.

In the first test, six stations of SURFRAD, a US network collecting well-calibrated ground measurements of surface SW albedo, were considered during 2018-2019 (Table II). The global upwelling and downwelling solar radiation fluxes (W/m^2) are recorded by upward and downward facing pyranometers placed on towers at the heights of 10 m. The downward pyranometers have a circular ground footprint of about a 60-m radius. Therefore, to compare satellite albedo retrievals with SURFRAD measurements, an 11×11 window size of Sentinel-2's 10-m pixels were considered to cover the pyranometer footprint. As in [21], a cosine-factor upscaling was used to aggregate the albedo values α of each pixel in the 11×11 window. Thus, the surface albedo α_{av} was obtained as a weighted average of the Sentinel-2 α at 10-m resolution

$$\alpha_{\text{av}} = \frac{\sum_{i=1}^{121} \cos(\beta_i) \cdot \alpha(i)}{\sum_{i=1}^{121} \cos(\beta_i)} \tag{3}$$

where β_i is the angle between the tower vertical and the line from pyranometers to the center of pixel i within the 11×11 grid area. Fig. 2 shows an example of Sentinel-2 albedo map.

The second test was performed over 18 ground points selected in a measurement campaign carried out in the Perugia urban area during summer 2016, described in [22]. An linear programming (LP) PYRA 05 albedometer with two upward and downward pyranometers was positioned at a height of 1.5 m. The downward pyranometers had a circular ground footprint of about 7-m radius. The selected points are characterized by a fairly homogenous surface, representing different types of artificial and natural urban surfaces, as detailed in [22] (different types of asphalt, sand, gravel, grass, bitumen, white tiles). The measured albedo values encompass a large range (0.111–0.455). In this second test, only Sentinel-2A data were considered, since Sentinel-2B was still not launched.

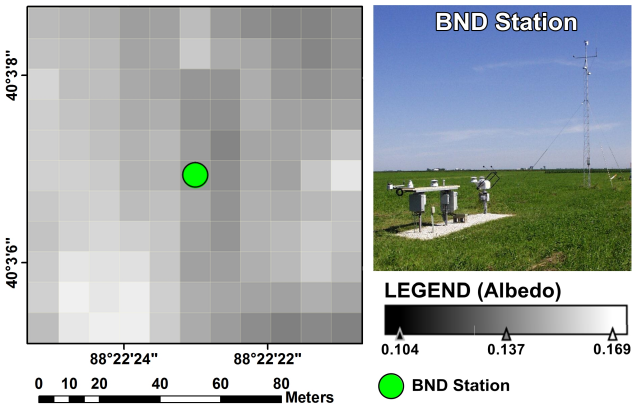

Fig. 2. BND SURFRAD station, 25 July 2019: 11×11 albedo map of Sentinel-2's 10-m pixels covering the BND pyranometer footprint.

III. RESULTS AND DISCUSSION

In literature, ground measurements of surface albedo by pyranometers have been used to assess satellite albedo retrievals across different spatial scales and methods [16], [21], [23]. In the narrow-to-broadband algorithm category, Liang coefficients [4] proved high accuracy over sites of soils, crops, and natural vegetation, with an average error of around 0.02 [23].

Retrieval of surface albedo from Landsat and Sentinel-2 (20–30-m resolution) applying anisotropy information from concurrent coarser resolution (500-m) MODIS BRDF products [7] was proposed in previous studies [15], [16], [21]. In these approaches, the narrow-to-broadband conversion is the main step before the BRDF application. However, the process of scaling MODIS BRDF to finer scales is not straightforward and requires homogeneous features inside the 500-m pixels [16], [20]. Therefore, the application of the BRDF modeling to heterogeneous areas, such as urban ones, is unadvisable.

As specified, this letter focuses on the accurate evaluation of the narrow-to-broadband albedo conversion. Albedo from ground pyranometers is the ratio of bi-hemispherical reflected and incident radiant flux. Satellite reflectivity observations correspond to hemispherical (incoming) - conical (reflected) radiation ratio [24]. For surfaces assumed roughly isotropic in reflectance, the satellite spectral reflectivity is converted into SW albedo by (1) without the necessity of BRDF modeling.

Altthough the Lambertian assumption may fail over different land covers, it will be considered valid in the

Authorized licensed use limited to: UNIVERSIDAD CARLOS III MADRID. Downloaded on October 05,2021 at 13:20:51 UTC from IEEE Xplore. Restrictions apply.

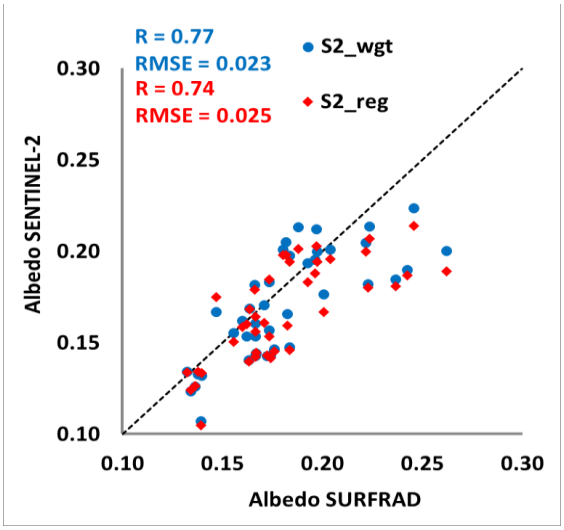

Fig. 3. Albedo measurements from SURFRAD stations versus Sentinel-2A/B albedo estimations by S2_wgt (blue) and S2_reg (red) methods.

following tests. In fact, as in [4], [22], and [23], the test surfaces are rough but without dominant 3-D structures, and the satellite data are acquired near midday, generally ensuring a large solar elevation angle. These conditions are essential for Lambertian surface approximation.

A. SURFRAD Test

SURFRAD instruments measure radiation fluxes every minute, and the average value of the measurements matching ±15 min with respect to the Sentinel-2 overpass time was considered. A total of 42 clear-sky images were selected; the local time of the satellite passages was around 11:00 A.M.

Fig. 3 shows the accuracy results of the two methods, both using 10-m pixel size, with respect to the corresponding SURFRAD measurements. The root-mean-square error (RMSE) and the correlation coefficient (R) between satellite retrievals and pyranometer measurements highlight the good performances of the two narrow-to-broadband conversion methods. Slightly better performance for S2_wgt in both RMSE and *R* is revealed, especially for the albedo values higher than 0.2 that the two methods tend to underestimate.

The RMSE is slightly above 0.02, and it is in line with the accuracy found over homogeneous rural sites by the Liang coefficients for satellite sensors having coarser resolutions [23]. Recent letters tested Sentinel-2 albedo retrievals over SURFRAD stations applying BRDF products. Franch *et al.* [15] used the Landsat ETM+ narrow-to-broadband coefficients for Sentinel-2 data with BRDF normalization and found the same accuracy of 0.02. Li *et al.* [16] used data from Sentinel-2A at 20-m pixel size, but without the weighting of (3). In [16], surface BRDF anisotropy information at a spatial scale of 500 m to 1 km was applied to Sentinel-2A reflectances, and accuracy between 0.023 and 0.026 was found. The satellite results of Fig. 3 are obtained assuming surfaces isotropic in reflectance, and the accuracy comparable to that of [15] and [16] seems to confirm that the assumption is not far from the actual situation.

Since test data encompass all the months during the years 2018 and 2019, Fig. 4 shows the albedo error percentage as a function of the solar elevation angle.

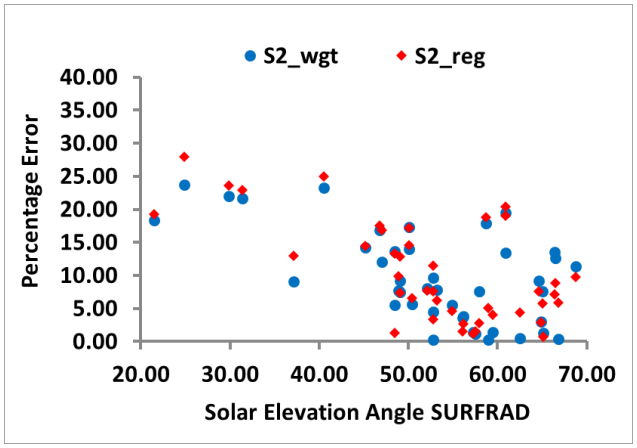

Fig. 4. Error percentage of the albedo from Sentinel-2A/B with respect to SURFRAD measurements as a function of the solar elevation angle.

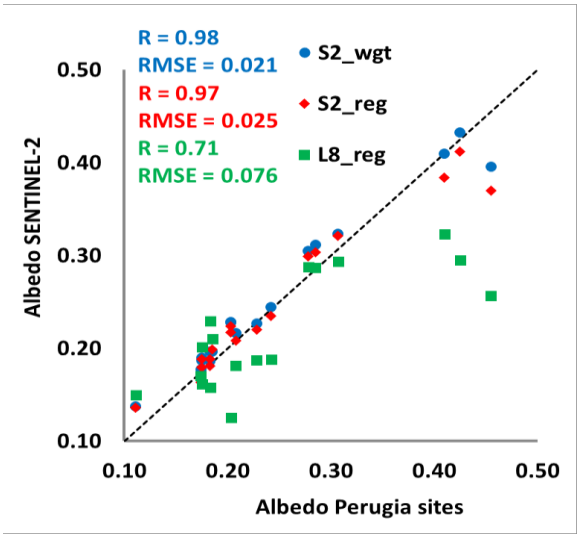

Fig. 5. Summer 2006: albedo measurements at Perugia sites versus albedo estimations from Sentinel-2A by S2_wgt (blue) and S2_reg (red) methods, and from Landsat 8 by Liang coefficients (L8_reg, green).

The outcomes point out how the lower solar elevation angles (December–February months) can be the most critical for the performance of the narrow-to-broadband coefficients. Since a condition for Lambertian assumption is a large solar elevation angle, at lower angles, this assumption is weak for the test sites, as evidenced by the increased retrieval error of the albedo.

Generally, the albedo variation with the sun elevation is more prominent for smooth soils with respect to rough surfaces, the latter with almost no albedo changes at solar elevation angles greater than 25°–30° [25].

B. Urban Test (Perugia)

The same time selection and averaging of SURFRAD test (±15 min around Sentinel-2 overpass time) was applied for the Perugia albedometer measurements (18 sites). The local time of satellite passages is around 12:00 A.M., and the Sentinel-2A 10-m pixel containing the instrument location was selected.

The *in situ* campaign was carried out in summer 2016 to assess the reliability of the albedo estimation by

Authorized licensed use limited to: UNIVERSIDAD CARLOS III MADRID. Downloaded on October 05,2021 at 13:20:51 UTC from IEEE Xplore. Restrictions apply.

narrow-to-broadband conversion coefficients using Landsat 8 operational land imager (OLI) data. This sensor observes reflectivities with a 30-m resolution, and the Liang coefficients [4] were used for albedo retrieval. Details on surface features of the 18 sites and Landsat 8 processing are provided in [22].

The S2_wgt and S2_reg performance over these sites, characterized by different types of artificial and natural urban surfaces assumed Lambertian [22], is then evaluated, as well as their accuracy with respect to Landsat 8 estimations.

Fig. 5 reports the albedo from S2_wgt, S2_reg (10-m), and Landsat 8 (L8_reg, 30-m). Sentinel-2 retrieval is better than Landsat 8, and again S2_wgt slightly outperforms S2_reg. For the highest albedo values (> 0.4), the improvement of Sentinel-2 with respect to Landsat 8 is very noticeable.

Albeit each site is fairly homogeneous [22], inside the Landsat 8 pixel, there might be the contamination of neighboring areas with different albedos. This test shows the advantage of using a finer resolution in urban areas and the reliability of the proposed coefficients for the Sentinel-2 data.

IV. Conclusion

The proposed narrow-to-broadband conversion coefficients provide good performance in the albedo retrieval from cloudless Sentinel-2 observations. The algorithm application requires that the surfaces are assumed as Lambertian. The accuracy is slightly better than the same approach with coefficients computed by regression. The albedo estimated with 10-m pixel size, exploiting a resolution enhancement method applied to the coarser SWIR pixels, is reliable and accurate also in urban environments, where BRDF modeling with satellite products is unadvisable. The availability of easy-to-use algorithms for satellite albedo retrieval in different environments roughly isotropic (quite rough but without dominant 3-D structures) represents a useful tool to quantify the surface solar-reflection properties continuously over time.

Acknowledgment

The authors would like to thank G. Baldinelli, A. Rotili, and J. Cancelloni for the Perugia *in situ* campaign.

References

[1] R. E. Dickinson, "Land surface processes and climate—Surface albedos and energy balance," *Adv. Geophys.*, vol. 25, pp. 305–353, 1983.

[2] S. Liang, K. Wang, X. Zhang, and M. Wild, "Review on estimation of land surface radiation and energy budgets from ground measurement, remote sensing and model simulations," *IEEE J. Sel. Top. Appl. Earth Observat. Remote Sens.*, vol. 3, no. 3, pp. 225–240, Sep. 2010.

[3] S. Bonafoni, G. Baldinelli, and P. Verducci, "Sustainable strategies for smart cities: Analysis of the town development effect on surface urban heat island through remote sensing methodologies," *Sustain. Cities Soc.*, vol. 29, pp. 211–218, Feb. 2017.

[4] S. Liang, "Narrowband to broadband conversions of land surface albedo I: Algorithms," *Remote Sens. Environ.*, vol. 76, pp. 213–238, May 2001.

[5] G. Baldinelli, S. Bonafoni, R. Anniballe, A. Presciutti, B. Gioli, and V. Magliulo, "Spaceborne detection of roof and impervious surface albedo: Potentialities and comparison with airborne thermography measurements," *Solar Energy*, vol. 113, pp. 281–294, Mar. 2015.

[6] Y. Qu, S. Liang, Q. Liu, T. He, S. Liu, and X. Li, "Mapping surface broadband albedo from satellite observations: A review of literatures on algorithms and products," *Remote Sens.*, vol. 7, no. 1, pp. 990–1020, Jan. 2015.

[7] B. Schaaf *et al.*, "First operational BRDF, albedo nadir reflectance products from MODIS," *Remote Sens. Environ.*, vol. 83, pp. 135–148, Nov. 2002.

[8] C. L. Brest and S. N. Goward, "Deriving surface albedo measurements from narrow band satellite data," *Int. J. Remote Sens.*, vol. 8, no. 3, pp. 351–367, Mar. 1987.

[9] M. J. Russell *et al.*, "Conversion of nadir, narrowband reflectance in red and near-infrared channels to hemispherical surface albedo," *Remote Sens. Environ.*, vol. 61, pp. 16–23, Jul. 1997.

[10] R. W. Saunders, "The determination of broad band surface albedo from AVHRR visible and near-infrared radiances," *Int. J. Remote Sens.*, vol. 11, no. 1, pp. 49–67, Jan. 1990.

[11] J. A. Valiente *et al.*, "Narrow-band to broad-band conversion for Meteosat-visiible channel and broad-band albedo using both AVHRR-1 and-2 channels," *Int. J. Remote Sens.*, vol. 16, no. 6, pp. 1147–1166, 1995.

[12] M. Tasumi, R. G. Allen, and R. Trezza, "At-surface reflectance and albedo from satellite for operational calculation of land surface energy balance," *J. Hydrol. Eng.*, vol. 13, no. 2, pp. 51–63, 2008.

[13] K. Naegeli, A. Damm, M. Huss, H. Wulf, M. Schaepman, and M. Hoelzle, "Cross-comparison of albedo products for glacier surfaces derived from airborne and satellite (Sentinel-2 and Landsat 8) optical data," *Remote Sens.*, vol. 9, no. 2, p. 110, Jan. 2017.

[14] F. Canisius *et al.*, "A UAV-based sensor system for measuring land surface albedo: Tested over a boreal peatland ecosystem," *Drones*, vol. 3, no. 1, p. 27, Mar. 2019.

[15] B. Franch, "A method for landsat and sentinel 2 (HLS) BRDF normalization," *Remote Sens.*, vol. 11, no. 6, p. 632, 2019.

[16] Z. Li *et al.*, "Preliminary assessment of 20-m surface albedo retrievals from sentinel-2A surface reflectance and MODIS/VIIRS surface anisotropy measures," *Remote Sens. Environ.*, vol. 217, pp. 352–365, Nov. 2018.

[17] *Sentinel-2 Missions and Multispectral Instrumen (MSI) Overview*. Accessed: Jun. 1, 2019. [Online]. Available: https://sentinel.esa.int/web/sentinel/user-guides/sentinel-2-msi

[18] *Colour Vision for Copernicus. The Story of Sentinel-2*. Accessed: Jun. 1, 2019. [Online]. Available: http://esamultimedia.esa.int/docs/EarthObservation/Sentinel-2_ESA_Bulletin161.pdf

[19] N. Brodu, "Super-resolving multiresolution images with band-independent geometry of multispectral pixels," *IEEE Trans. Geosci. Remote Sens.*, vol. 55, no. 8, pp. 4610–4617, Aug. 2017.

[20] C. Gueymard, "SMARTS2: A simple model of the atmospheric radiative transfer of sunshine: Algorithms and performance assessment," Florida Solar Energy Center, Univ. Central Florida, Cocoa, FL, USA, Prof. Paper FSEC-PF-270-95, 1995.

[21] Y. Shuai, J. G. Masek, F. Gao, and C. B. Schaaf, "An algorithm for the retrieval of 30-m snow-free albedo from Landsat surface reflectance and MODIS BRDF," *Remote Sens. Environ.*, vol. 115, no. 9, pp. 2204–2216, Sep. 2011.

[22] G. Baldinelli, S. Bonafoni, and A. Rotili, "Albedo retrieval from multispectral landsat 8 observation in urban environment: Algorithm validation by *in situ* measurements," *IEEE J. Sel. Topics Appl. Earth Observ. Remote Sens.*, vol. 10, no. 10, pp. 4504–4511, Oct. 2017.

[23] S. Liang *et al.*, "Narrowband to broadband conversions of land surface albedo: II. Validation," *Remote Sens. Environ.*, vol. 84, no. 1, pp. 25–41, Jan. 2003.

[24] G. Schaepman-Strub, M. E. Schaepman, T. H. Painter, S. Dangel, and J. V. Martonchik, "Reflectance quantities in optical remote sensing—Definitions and case studies," *Remote Sens. Environ.*, vol. 103, pp. 27–42, Jul. 2006.

[25] J. Cierniewski *et al.*, "Effects of soil surface irregularities on the diurnal variation of soil broadband blue-sky albedo," *IEEE J. Sel. Top. Appl. Earth Observ. Remote Sens.*, vol. 8, no. 2, pp. 493–502, Feb. 2015.

Authorized licensed use limited to: UNIVERSIDAD CARLOS III MADRID. Downloaded on October 05,2021 at 13:20:51 UTC from IEEE Xplore. Restrictions apply.